Title

High fluence light emitting diode-generated red light modulates characteristics associated with skin fibrosis.

Journal

Journal of biophotonics, 9(11-12)

ISSN

1864-063X

Authors

Mamalis, Andrew
Koo, Eugene
Garcha, Manveer
et al.

Publication Date

2016-12-01

DOI

10.1002/jbio.201600059

Peer reviewed

HHS Public Access

Author manuscript

J Biophotonics. Author manuscript; available in PMC 2017 December 01.

Published in final edited form as:

J Biophotonics. 2016 December ; 9(11-12): 1167–1179. doi:10.1002/jbio.201600059.

High Fluence Light Emitting Diode-Generated Red Light Modulates Characteristics Associated with Skin Fibrosis

Andrew Mamalis[1,2], **Eugene Koo**[1,2], **Manveer Garcha**[1], **William J. Murphy**[1], **R. Rivkah Isseroff**[1,2], and **Jared Jagdeo**[1,2,3]

[1]Department of Dermatology, University of California at Davis, Sacramento, CA, USA

[2]Dermatology Service, Sacramento VA Medical Center, Mather, CA, USA

[3]Department of Dermatology, SUNY Downstate, Brooklyn, NY, USA

Abstract

Skin fibrosis, often referred to as skin scarring, is a significant international health problem with limited treatment options. The hallmarks of skin fibrosis are increased fibroblast proliferation, collagen production, and migration speed. Recently published clinical observations indicate that visible red light may improve skin fibrosis. In this study we hypothesize that high-fluence light-emitting diode-generated red light (HF-LED-RL) modulates the key cellular features of skin fibrosis by decreasing cellular proliferation, collagen production, and migration speed of human skin fibroblasts. Herein, we demonstrate that HF-LED-RL increases reactive oxygen species (ROS) generation for up to 4 hours, inhibits fibroblast proliferation without increasing apoptosis, inhibits collagen production, and inhibits migration speed through modulation of the phosphoinositide 3-kinase (PI3K)/Akt pathway. We demonstrate that HF-LED-RL is capable of inhibiting the unifying cellular processes involved in skin fibrosis including fibroblast proliferation, collagen production, and migration speed. These findings suggest that HF-LED-RL may represent a new approach to treat skin fibrosis. LED advantages include low cost, portability, and ease of use. Further characterizing the photobiomodulatory effects of HF-LED-RL on fibroblasts and investigating the anti-fibrotic effects of HF-LED-RL in human subjects may provide new insight into the utility of this therapeutic approach for skin fibrosis.

Introduction

Skin fibrosis, often referred to as skin scarring, is a significant international health problem, with an estimated incidence of greater than 100 million persons affected per annum worldwide [1, 2]. The hallmarks of skin fibrosis are increased fibroblast proliferation, collagen production, and migration speed [3-5]. Skin fibrosis is involved in a variety of pathologic processes ranging from excess scar formation in keloid scars to immune-mediated scarring processes such as scleroderma and chronic graft versus host disease [3].

Corresponding author: Jared Jagdeo, MD, MS, jrjagdeo@gmail.com, Telephone: (917) 837-9796, Fax: (916) 451-7245.

The content is solely the responsibility of the authors and does not necessarily represent the official views of the National Institutes of Health.

PhotoTherapeutics provided the device used in this study.

Although skin fibrosis imparts a significant socioeconomic burden, there are limited cost-effective, non-invasive therapeutic modalities. Current skin fibrosis treatments typically require expensive pharmacologic, surgical, or invasive treatments associated with a significant risk of side effects. Even with combination therapy and a good treatment outcome, skin fibrosis frequently recurs [6, 7].

Ultraviolet (UV) phototherapy is sometimes used to treat skin fibrosis associated with various diseases. However, UV irradiation causes thymidine dimer DNA damage that is associated with increased rates of skin cancers and premature photoaging [8-10]. Furthermore, UV phototherapy can be expensive, inconvenient, and burdensome to patients due to frequent office visits, and is not readily available for home use [11, 12]. In contrast, light-emitting diode-generated red light (LED-RL) phototherapy is a safe, non-invasive, inexpensive, and portable treatment that can be used at home and combined with existing treatment modalities. For these reasons, HF-LED-RL has the potential to change the treatment paradigm of fibrotic skin disease.

Visible light is ubiquitous in our environment and accounts for 44% of total solar energy, however, its effects on skin function and physiology have not been well characterized [13]. Visible light is a potentially safer therapeutic option compared to UV light since visible light does not generate DNA damage associated with skin cancer [13]. Recently published clinical observations indicate that red light, in combination with other modalities, may improve skin fibrosis [14-16]. These findings suggest that visible red light and its effects on the cellular function of skin fibroblasts are worthy of further scientific investigation if it is to be utilized in the treatment of skin fibrosis as the effects of LED-RL on human dermal skin fibroblasts (HDFs) are not well characterized.

Our group previously demonstrated that high fluence LED-RL (HF-LED-RL; defined as equal to or greater than 160 J/cm^2) is capable of decreasing the cell counts of treated HDFs compared to untreated controls [17]. In this study we hypothesize that HF-LED-RL modulates the key cellular features of skin fibrosis by decreasing cellular proliferation, collagen production, and migration speed of HDFs. Herein, we demonstrate that HF-LED-RL increases reactive oxygen species (ROS) generation, inhibits HDF proliferation without increasing apoptosis, inhibits collagen production, and decreases HDF migration speed through modulation of the PI3K/Akt pathway.

Materials and Methods

Materials

Tissue culture dishes (35-mm) were purchased from Corning Life Sciences (Tewksbury, MA). The Dulbecco's Modified Eagle's Medium, CO_2-independent medium, fetal bovine serum, phosphate buffered saline (PBS), and antibiotic-antimycotic mixture (penicillin, streptomycin, and amphotericin B) were from Invitrogen Life Technology (Invitrogen, Carlsbad, CA). The picric acid and sirius red dye were obtained from Sigma-Aldrich (St. Louis, MO). The PI3K/Akt inhibitor LY294002 and antibodies against total and phosphorylated forms of Akt (Ser473) and Erk1/2 (Thr202/Tyr204) were from Cell

Signaling (Beverly, MA). Dihydrorhodamine (DHR) was from Calbiochem/Millipore (San Diego, CA).

LED Array Characteristics

The light source used was a commercially available Omnilux New-U hand held LED array (PhotoTherapeutics, CA). This LED unit has a 4.7 cm × 6.1 cm rectangular aperture and emits visible red light (633 nm ± 30 nm) at a power density of 360.2 W/m^2 at room temperature and a distance of 10 mm from the bottom of the tissue culture dish to the LED array [17, 18].

Cell Culture

Commercially available, normal human dermal fibroblasts cultures (AG13145) were maintained at 37°C in 5% CO2 with Dulbecco's Modified Eagle Medium, 10% FBS, 1% antibiotic as previously described [17]. For experiments, fibroblasts were plated at 2×10^4 cells per 35-mm dish. All experiments were performed on cell cultures passage 12 or less and were repeated to verify data reproducibility and accuracy. Similar trends were demonstrated in a second primary human skin fibroblast culture (NHF05-01) isolated from a different patient under an IRB-approved protocol.

HDF Irradiation

HDFs were seeded at 2×10^4 cells per 35-mm tissue culture dish, incubated for 24 hours, and then irradiated using the aforementioned LED source. To ensure the effects measured were not the result of thermal output of the LED array, media temperatures, measured by a probe thermometer, were maintained between 32-34°C as previously described [17, 18]. This ensured that HDFs remained within a physiologic temperatures range throughout treatment.

Each experimental condition receiving HF-LED-RL treatment had a temperature-matched sham-irradiated control to ensure that the measured effect was the result of LED treatment and not due to ambient light or environment. Controls were derived from the same stock of cell suspension, taken out of the incubator at the same time as their matched treatment pairs, were protected from the LED light source, placed on a digital warming block with a negative feedback temperature control system set at 32°C. Similar to treated cultures, control media temperatures measured throughout irradiation remained 32-34°C.By remaining within physiologic temperature range, heat stress was not induced.

Following irradiation, experimental and matched control dishes were returned to the incubator and then harvested for relevant assays at the appropriate time-course. Doses for irradiation were selected based upon our pilot irradiation studies and prior studies [17, 19].

Trypan Blue Cell Counts

To assess HF-LED-RL effects on cell count, HDF cultures were irradiated with HF-LED-RL as described above, and cells were counted as previously described [17]. Briefly, 48 hours after irradiation, cell counts were taken that included all cells in the sample, including media change, trypsinization products, and washes. Cells counts were calculated by sampling a

known volume (10 μL) and measuring the cell concentration using a hemocytometer and trypan blue.

Tritiated Thymidine Proliferation Assay

To assess HF-LED-RL effects on proliferation, HDF cultures were irradiated with HF-LED-RL as described above, and proliferation was assessed using the tritium incorporation assay as previously described [20, 21]. Briefly, immediately following HF-LED-RL treatment, cells were pulsed with 4 μCi/mL of tritiated thymidine (3H-Thy). The dishes were then incubated for 18 hours, cells were collected, and counted on a scintillation beta-counter. The results are expressed as the relative percent counts per minute ± percent standard error of the mean.

Gross Cellular Morphology

To assess HF-LED-RL effects on cellular morphology, HDF cultures were irradiated with HF-LED-RL as described above and cellular morphology was observed for 12 hours post-irradiation for alterations using a time-lapse video microscope. For purposes of comparison, we used LED blue light (415 nm) at 80 and 160 J/cm^2 and 1.2 mM H_2O_2 as positive controls that all induced alterations in cellular morphology.

Flow Cytometry-Based Apoptosis/Necrosis and Reactive Oxygen Species Assays

Flow cytometry data acquisition was performed on a BD FACSCalibur flow cytometer. HDF cultures were irradiated with HF-LED-RL as described above. To assess cells for increases in apoptosis, following treatment with HF-LED-RL, HDFs were trypsinized, collected, and resuspended with 3 μL of 7-amino-actinomycin D (7-AAD; BD Biosciences) and 1 μL of Annexin V (AV; BD Biosciences) in 96 μL of PBS. FlowJo (TreeStar, Inc.) software was used to gate on the AV^+ $7AAD^-$ and AV^+ $7AAD^+$ populations.

Cells were assessed for intracellular ROS generation as previously described [22]. Briefly, 2 × 10^4 cells per 35-mm dish were intravitally stained with dihydrorhodamine at 30 μM and then irradiated as described above. Following irradiation, cells were collected and analyzed by flow cytometry. FlowJo software was used to calculate mean fluorescent intensity of DHR.

Time-Lapse Video Cell Migration Microscopy

Time-lapse video migration experiments were performed as previously described with modifications [23]. For migration experiments, primary HDFs were plated on 35-mm culture dishes with CO_2-independent medium and incubated for 24 hours. In some experiments, HDFs were pretreated with LY294002, a selective PI3K/Akt inhibitor, as described below. Cells were irradiated as described above. Following irradiation, time-lapse images of the cell migration were captured every 30 minutes for 4 hours in an environmental chamber monitored under microscopy with the temperature maintained at 37 °C. The time-lapse videos were generated using Volocity Image Software (PerkinElmer) and were analyzed using Openlab Software (PerkinElmer) to measure cell migration speed in micrometers per minute that the cells travel over a 4-hour period.

LY294002 Small Molecule Inhibitor

Cells were pretreated with 30 μM of LY294002 for 30 minutes prior to irradiation. Cells were irradiated, and then time-lapse video migration experiments were performed as described above.

Picrosirius Red Staining Quantification and Visualization of Collagen

Picrosirius red (PSR) staining solution used in staining collagen was made from 0.1% (weight/volume) picrosirius red dye (Sigma-Aldrich) in a saturated picric acid solution. In brief, cells were cultured and irradiated as described above. 48 hours following HF-LED-RL irradiation, cells were fixed in 4% paraformaldehyde at room temperature for 15 minutes, then washed twice with PBS. Cells were then stained with the PSR staining solution for 90 minutes at 37°C. The staining solution was removed and the cells were washed three times with acidified water (0.25% acetic acid). For quantitative analysis, PSR stain was eluted from cells using 200 μL of 0.1 M NaOH, collected in a 96-well microplate, and 540-nm absorbance was read using a Bio-Rad microplate reader.

For light microscopy visualization of collagen staining, cells were cultured on glass coverslips and then stained with picrosirius red solution as described above. Coverslips were mounted with Permount (Electron Microscopy Sciences, USA). The slides were examined and representative photographs were taken at 40× magnification using a BioRevo BZ-9000 microscope (Keyence, Osaka, Japan). Photographs were taken at an exposure of $1/15^{th}$ of a second and white-balanced using the BioRevo Image Analysis software.

Western Blot

Following irradiation, HDFs were rinsed with ice-cold PBS and scraped in 25 μl NP40 cell lysis buffer (Invitrogen) with 1× Protease inhibitor cocktail (Sigma-Aldrich) and 1mM phenylmethylsulfonyl fluoride (PMSF) (Sigma-Aldrich). Cell lysates vortexed and then spun at 12,000 rpm at 4°C for 10 minutes and the supernatants were stored at −80°C. Protein concentration in the lysates was determined by Bio-Rad protein assay (Bio-Rad, Hercules, CA) and 20 μg protein from each sample was loaded. Gel Electrophoresis was performed with NuPAGE® Novex Gel Electrophoresis system (4–12% gels, Invitrogen) and transferred onto polyvinylidene difluoride (PVDF) membranes for Western blotting. PVDF membranes were blocked with Odyssey blocking buffer (LI-COR Biosciences) and then incubated with primary antibodies overnight at 4°C. Afterward, PVDF membranes were washed and incubated with IRDye infrared secondary antibodies (LI-COR Biosciences, Lincoln, NE) for 1 hour at room temperature. Protein bands on the blots were scanned with an Oddyssey Fc Imager (LI-COR Biosciences) and quantified using the ImageStudio program (LI-COR Biosciences). Antibodies against total and phosphorylated forms of Akt (Ser473) and Erk1/2 (Thr202/Tyr204) (Cell Signaling) were used at 1:1,000 dilutions. The antibody against procol1A1 (Santa Cruz Biotechnology, CA) was used at a 1:100 dilution. The antibody against Anti-GAPDH (Millipore) was used at 1:10,000. Secondary antibodies were used at 1:10,000 dilutions.

Statistical Analysis

Statistical analyses with analysis of variance (ANOVA) and Student's t-test were performed using GraphPad Prism version 6.00 for OSX (GraphPad Software, San Diego, CA, USA) to compare HF-LED-RL irradiated cells with matched controls. The significance level was set at $p < 0.05$. The paired study design and sample sizes were chosen under the supervision of a biostatistician.

Results

HF-LED-RL inhibits proliferation without increasing apoptosis levels

We have previously demonstrated that treating HDFs with HF-LED-RL results in decreases in cell count 48 hours after irradiation using a trypan blue exclusion assay [17]. Using this same assay, we found that 24 hours after irradiation, 640, but not 320 J/cm^2, LED-RL resulted in a significant decrease in cell count (Figure 1a). 48 hours after irradiation, cells counts of HDFs treated with 320 or 640 J/cm^2 were significantly decreased compared to matched controls (Figure 1a). Additionally, we found that multiple doses of HF-LED-RL (4 doses, once every 12 hours, over a 48 hour period) resulted in further decrease in cell count compared to matched controls (Figure 1b).

To determine if these decreases in cell count are due to HF-LED-RL decreasing proliferation rate, HDFs were irradiated with HF-LED-RL and then incubated with tritiated thymidine (3H-Thy). Incorporation of 3H-Thy was measured to quantify DNA synthesis, a surrogate of cellular proliferation. Treatment with 320 and 640 J/cm^2 LED-RL led to significantly decreased proliferation rates of 84% and 33% relative to matched control HDFs, respectively (Figure 1c).

To determine if HF-LED-RL led to immediate or delayed increases in cellular apoptosis, HDFs were irradiated with HF-LED-RL. At 0, 2, and 4 hours after irradiation, apoptosis levels were quantified using flow cytometry. Annexin V (AV)-positive populations were measured and compared with matched controls. 320 and 640 J/cm^2 LED-RL irradiations did not significantly increase total cellular apoptosis levels at 0, 2, or 4 hours post-irradiation compared to controls. (Figure 1d, 1e).

HF-LED-RL does not alter gross morphology of HDFs

When HDFs and other cells are exposed to low doses of UVB-irradiation (280-320 nm), changes in cellular morphology are evident within 2 hours after irradiation [24, 25]. To determine if HF-LED-RL also led to any gross abnormalities in cellular morphology, HDFs were irradiated with 320 and 640 J/cm^2 LED-RL and then imaged at 0, 4, 8, and 12 hours post-irradiation using a video microscope. We found no difference in cellular morphology between HF-LED-RL treated cells and matched control cells (Supplemental Figure 1a). In contrast, altered morphology was observed in positive control samples following treatment with 80 and 160 J/cm^2 of visible LED blue light (415 nm) that is near the UV spectrum, and positive control samples treated with 1.2 mM H_2O_2 for 1 hour. Additionally, while multiple doses of HF-LED-RL (4 doses, once every 12 hours, over a 48 hour period) did not alter

gross HDF morphology, it did result in a difference in total cell count 48 hours post irradiation when cells were viewed by video microscopy (Supplemental Figure 1b).

HF-LED-RL increases ROS generation for up to 4 hours following irradiation

Broad-spectrum (400-700 nm) visible light is reported to lead to significant increases in ROS generation that are hypothesized to play a role in light-associated alterations in cellular physiology [13]. To determine if HF-LED-RL associated increases in ROS are sustained for up to 4 hours following irradiation, HDF cultures were irradiated with 320 and 640 J/cm^2 LED-RL and ROS levels were measured using flow cytometry. At 0, 1, 2, and 4 hours following irradiation, ROS levels were significantly elevated compared to matched controls. Peak ROS levels were observed 1 hour following 320 and 640 J/cm^2 LED-RL and found to be 127% and 145% relative to matched control, respectively (Figure 2a and 2b). No further increases in ROS levels were noted at later time points.

LED-RL significantly inhibits HDF collagen production

Given that an increased collagen level is a fundamental alteration seen in skin fibrosis, we next investigated the effects of HF-LED-RL on HDF collagen production. To measure the effect of HF-LED-RL on collagen production, cultures were irradiated, fixed, and stained with picrosirius red, a dye specific for collagen. Spectrophotometric analysis demonstrated a dose-dependent decreases in collagen levels 48 hours by 16.8% and 45.9% following 320 and 640 J/cm^2 LED-RL irradiation, respectively (Figure 3a). Furthermore, light microscopy demonstrated a qualitative decrease in collagen staining 48 hours following HF-LED-RL (Figure 3b). Additionally, we quantified procollagen 1A1 levels, the primary precursor of collagen type 1, at 0 and 2 hours following irradiation with LED-RL. Western blots of HDF protein lysates 0 hours after irradiation did not demonstrate a decrease in procollagen 1A1 levels. However, 2 hours following irradiation, HDF lysates demonstrated a significant decrease in the levels of procollagen 1A1 (Figure 3c, 3d) suggesting that HF-LED-RL associated decreases in collagen content may be due to decreases in collagen production.

LED-RL induced inhibition of HDFs migration speed is dose dependent and lasts up to 12 hours

HDF migration speed has been hypothesized to play a key role in the pathogenesis of skin fibrosis [4, 5]. To investigate the effects of HF-LED-RL on migration speed, HDFs were irradiated with 320 and 640 J/cm^2 of LED-RL, and cellular migration speed was measured using time-lapse video microscopy (Figure 4a). HDF migration speed was significantly inhibited in a dose-dependent manner. To further characterize the duration-of-effect of HF-LED-RL on migration speed, we demonstrated that 320 and 640 J/cm^2 of LED-RL significantly inhibited HDF migration speed for up to 12 hours post-irradiation (Figure 4b; a representative full 24-hour time course is presented in Supplemental Figure 2).

LED-RL alters migration speed through modulation of the PI3K/Akt pathway, but not the MAPK/ERK pathway

The PI3K/Akt and MAPK/ERK pathways play crucial roles in the regulation of HDF migration [26, 27]. To determine if HF-LED-RL modulates these signaling pathways,

protein lysates from HDFs irradiated with 320 and 640 J/cm^2 LED-RL were analyzed using Western blot. HF-LED-RL did not lead to alterations in phospho-ERK or total ERK levels at 4 or 12 hours following irradiation (Supplemental Figure 3). However, 320 and 640 J/cm^2 of LED-RL led to increased phospho-Akt (S473) levels (Figure 4c and 4d) without altering total Akt levels (data not shown).

To determine if this modulation of the PI3K/Akt pathway led to the observed inhibition of HDF migration speed, the effects of 640 J/cm^2 LED-RL on migration speed were measured following pretreatment with 30 μM of LY294002, a small molecule inhibitor of Akt phosphorylation. Pretreatment of control cells with LY294002 did not significantly change migration speed compared to untreated control cells (Figure 4e). Pretreatment of irradiated cells with LY294002 completely reversed the inhibitory effects of 640 J/cm^2 LED-RL resulting in a migration speed equal to that of matched controls (Figure 4f). These findings suggest that HF-LED-RL inhibition of HDF migration speed may be due to modulation of the PI3K/Akt pathway.

Discussion

HDF proliferation plays an important role in the initiation and propagation of skin fibrosis [1, 3]. Our study results demonstrate that HF-LED-RL modulates key cellular functions associated with skin fibrosis. We found that HF-LED-RL significantly decreased HDF cell count 48 hours after irradiation (Figure 1b) and this effect was augmented when HDFs were irradiated with multiple doses of HF-LED-RL. Further, we found that HF-LED-RL significantly inhibited HDF proliferation without a significant increase in apoptosis levels or an alteration in gross cellular morphology (Figure 1a-e and Supplemental Figure 1). Our 24-hour post-irradiation cell count data likely does not capture the significance of this inhibition on proliferation as it may be too early to evaluate cell count as a surrogate of proliferation. It has been reported that broad-spectrum (400-700 nm) visible light leads to generation of ROS responsible for many of the photobiomodulatory effects of visible light [13]. Our data demonstrate that visible HF-LED-RL generates significant increase in ROS that are still sustained at 4 hours after irradiation (Figure 2a and 2b). We hypothesize that these increases in ROS may play a role in initiating the photobiomodulatory effects of HF-LED-RL and further investigation is warranted. We recently demonstrated that the antioxidant resveratrol is capable of preventing the photobiomodulatory effects of HF-LED-RL on HDF migration [28].

Perhaps most fundamental to skin fibrosis pathology, using a picrosirius red collagen assay, we demonstrate that HF-LED-RL is capable of decreasing production of collagen by HDFs. The observed decrease in collagen is not simply due to decreased cell number in HF-LED-RL treated samples, as the decrease in collagen was greater than the observed decrease in HDF cell count. The change in total collagen levels is further supported by our finding that levels of procol1A1, the key precursor of collagen I, are decreased following HF-LED-RL irradiation. This is significant because an increased amount of collagen in skin is a unifying characteristic of all forms of skin fibrosis and a fundamental target that many treatments seek to address [3]. However, it is unclear to what degree these decreases in procol1A1 levels are solely contributing to our observed alterations in picrosirius red-measured total

collagen levels. Other researchers have demonstrated that LED-RL additionally has other effects on collagen homeostasis, including altering matrix metalloproteinase expression levels [29]. Further investigation is warranted to identify additional mechanisms that may contribute to HF-LED-RL associated decreases in collagen production or alterations in collagen homeostasis.

Furthermore, fibroblast migration speed is hypothesized to play a key role in the pathogenesis of skin fibrosis, possibly through the recruitment of deeper dermal fibroblasts to fibrotic sites [4, 5]. Our findings demonstrate that HF-LED-RL decreases the migration speed of HDFs for up to 12 hours post-irradiation (Figure 3A, 3B, and Supplemental Figure 2), suggesting that the effects of HF-LED-RL may be transient and may necessitate repeat treatments when translated to clinical trials. Prior studies have demonstrated that the PI3K/Akt and MAPK/ERK pathways play crucial roles in the regulation of fibroblast migration [26, 27, 30-32] and that visible LED light is capable of activating or inhibiting the phosphorylation state of key cell signaling molecules [33, 34]. While HF-LED-RL did not appear to alter phosphor-ERK signaling (Supplemental Figure 3), HF-LED-RL did significantly increase phospho-Akt levels (Figure 4c). Although increases in phospho-Akt is at times associated with increases in migration speed [35], the Akt pathway's role in regulating cell motility and cytoskeletal structure is not completely understood and instances of increased Akt phosphorylation also result in decreased migration speeds [35-37]. Similar to our findings, other researchers demonstrated that phospho-Akt upregulation may lead to decreased HDF migration speed [26] and the PI3K/Akt inhibitor, LY294002, blocks anti-migratory states associated with increased phospho-Akt [26]. In this study, we demonstrated that pretreatment of cells with the PI3K/Akt inhibitor LY294002 abolished HF-LED-RL's inhibitory effect on HDF migration (Figure 4e). These findings reveal a potential mechanism for how HF-LED-RL-modulated Akt signaling decreases HDF migration.

In vitro models of skin fibrosis are limited and even fibroblasts derived from fibrosis-associated tissue may not completely recapitulate the complex pathologic physiology. Therefore, we used normal HDF as in culture they proliferate until becoming contact inhibited and likely correlate to clinical fibrotic disease. One challenge of *in vitro* photobiology studies is ensuring that the measured effects are not simply due to temperature or environmental conditions; to address this concern in our study, each experimental culture receiving HF-LED-RL was compared with a temperature-matched control plate to ensure that the measured effect was the result of HF-LED-RL treatment and not due to ambient light, environment, or temperature. Furthermore, while LY294002 has a high degree of specificity for PI3K/Akt, it may not be exclusively selective for the PI3K/Akt pathway and may also act on apparently unrelated proteins [38].

Animal studies investigating the effects of HF-LED-RL on models of skin fibrosis may lend clinical support to these in vitro findings or reveal targets with therapeutic potential to treat skin fibrosis. We believe our use of commercially available LEDs as a visible light source is a strength of our study as other researchers may utilize these arrays for photobiomodulation research. There is currently a paucity of clinical data evaluating the safety of LED red light exposure at high fluences or its clinical effects on skin fibrosis.[39, 40] For translational researchers, our finding that changes in migration speed last for up to 12 hours implicates a

12-hour interval as a potential candidate dosing-interval schedule for future *in vivo* studies on HF-LED-RL.

Conclusion

Current therapeutic options for skin fibrosis remain limited. We demonstrate that HF-LED-RL is capable of inhibiting the unifying cellular processes involved in skin fibrosis including proliferation, migration, and collagen production *in vitro*. These findings suggest that HF-LED-RL may represent a paradigm shifting approach to altering HDF function for treatment of skin fibrosis.

LEDs warrant further clinical investigation as their advantages include low cost, portability, ease of use at home, low-energy consumption, and long lifespan of diode light sources. The evolution of LED-based device therapy is trending from in-office treatment with large, expensive, space occupying light devices to safe, less costly, portable, home use light devices. We anticipate that the number of patients that are treated out of office will eventually exceed the number of patient procedures performed in-office. Further research is warranted to identify the precise mechanisms and pathway alterations that contribute to HF-LED-RL associated decreases in collagen production as this may reveal potential molecular targets for treating fibrosis in areas not amenable to phototherapy. We hope to translate these efforts clinically, by performing Phase I and Phase II clinical trials in the near future. Further characterizing the photobiomodulatory effects of HF-LED-RL on HDFs and investigating the anti-fibrotic effects of HF-LED-RL in human subjects may provide new insight into the utility of this therapeutic approach for treatment of skin fibrosis.

Supplementary Material

Refer to Web version on PubMed Central for supplementary material.

Acknowledgments

Funding Source: The project described was supported by the National Center for Advancing Translational Sciences, National Institutes of Health, through grant number UL1 TR000002 and linked awards TL1 TR000133 and KL2 TR000134.

References

1. Bayat A, McGrouther DA, Ferguson MW. Skin scarring. BMJ. 2003; 326:88–92. [PubMed: 12521975]
2. Lim AF, Weintraub J, Kaplan EN, et al. The embrace device significantly decreases scarring following scar revision surgery in a randomized controlled trial. Plast Reconstr Surg. 2014; 133:398–405. [PubMed: 24105084]
3. Wynn TA, Ramalingam TR. Mechanisms of fibrosis: therapeutic translation for fibrotic disease. Nat Med. 2012; 18:1028–40. [PubMed: 22772564]
4. Wu CS, Wu PH, Fang AH, et al. FK506 inhibits the enhancing effects of transforming growth factor (TGF)-beta1 on collagen expression and TGF-beta/Smad signalling in keloid fibroblasts: implication for new therapeutic approach. Br J Dermatol. 2012; 167:532–41. [PubMed: 22540338]
5. Ashcroft KJ, Syed F, Bayat A. Site-Specific Keloid Fibroblasts Alter the Behaviour of Normal Skin and Normal Scar Fibroblasts through Paracrine Signalling. PLoS One. 2013; 8:e75600. [PubMed: 24348987]

6. Mamalis AD, Lev-Tov H, Nguyen DH, et al. Laser and light-based treatment of Keloids - a review. J Eur Acad Dermatol Venereol. 2013
7. Vitiello M, Abuchar A, Santana N, et al. An Update on the Treatment of the Cutaneous Manifestations of Systemic Sclerosis: The Dermatologist's Point of View. J Clin Aesthet Dermatol. 2012; 5:33–43.
8. Berking C, Takemoto R, Satyamoorthy K, et al. Induction of melanoma phenotypes in human skin by growth factors and ultraviolet B. Cancer Res. 2004; 64:807–11. [PubMed: 14871803]
9. Cleaver JE, Crowley E. UV damage, DNA repair and skin carcinogenesis. Front Biosci. 2002; 7:d1024–43. [PubMed: 11897551]
10. Matsumura Y, Ananthaswamy HN. Short-term and long-term cellular and molecular events following UV irradiation of skin: implications for molecular medicine. Expert Rev Mol Med. 2002; 4:1–22.
11. Koek MB, Sigurdsson V, van Weelden H, et al. Cost effectiveness of home ultraviolet B phototherapy for psoriasis: economic evaluation of a randomised controlled trial (PLUTO study). BMJ. 2010; 340:c1490. [PubMed: 20406865]
12. NPF. National Psoriasis Foundation Policy Brief: Phototherapy copayments impact access to treatment 2010 [cited 2015 10-10-2015]. Available from: http://www.psoriasis.org/document.doc?id=1387
13. Liebel F, Kaur S, Ruvolo E, et al. Irradiation of skin with visible light induces reactive oxygen species and matrix-degrading enzymes. J Invest Dermatol. 2012; 132:1901–7. [PubMed: 22318388]
14. Nie Z. Is photodynamic therapy a solution for keloid? G Ital Dermatol Venereol. 2011; 146:463–72. [PubMed: 22095178]
15. Sakamoto FH, Izikson L, Tannous Z, et al. Surgical scar remodelling after photodynamic therapy using aminolaevulinic acid or its methylester: a retrospective, blinded study of patients with field cancerization. Br J Dermatol. 2012; 166:413–6. [PubMed: 21848691]
16. Campbell SM, Tyrrell J, Marshall R, et al. Effect of MAL-photodynamic therapy on hypertrophic scarring. Photodiagnosis Photodyn Ther. 2010; 7:183–8. [PubMed: 20728843]
17. Lev-Tov H, Mamalis A, Brody N, et al. Inhibition of fibroblast proliferation in vitro using red light-emitting diodes. Dermatol Surg. 2013; 39:1167–70. [PubMed: 23590233]
18. Mamalis AD, Lev-Tov H, Nguyen DH, et al. Laser and light-based treatment of Keloids--a review. J Eur Acad Dermatol Venereol. 2014; 28:689–99. [PubMed: 24033440]
19. Mamalis A, Jagdeo J. Light-Emitting Diode-Generated Red Light Inhibits Keloid Fibroblast Proliferation. Dermatol Surg. 2014
20. Taub DD, Murphy WJ, Asai O, et al. Induction of alloantigen-specific T cell tolerance through the treatment of human T lymphocytes with wortmannin. J Immunol. 1997; 158:2745–55. [PubMed: 9058809]
21. Turcovski-Corrales SM, Fenton RG, Peltz G, et al. CD28:B7 interactions promote T cell adhesion. Eur J Immunol. 1995; 25:3087–93. [PubMed: 7489747]
22. Jagdeo J, Adams L, Lev-Tov H, et al. Dose-dependent antioxidant function of resveratrol demonstrated via modulation of reactive oxygen species in normal human skin fibroblasts in vitro. J Drugs Dermatol. 2010; 9:1523–6. [PubMed: 21120261]
23. Chen J, Hoffman BB, Isseroff RR. Beta-adrenergic receptor activation inhibits keratinocyte migration via a cyclic adenosine monophosphate-independent mechanism. J Invest Dermatol. 2002; 119:1261–8. [PubMed: 12485426]
24. Clydesdale GJ, Dandie GW, Muller HK. Ultraviolet light induced injury: immunological and inflammatory effects. Immunol Cell Biol. 2001; 79:547–68. [PubMed: 11903614]
25. Kurimoto I, Streilein JW. Deleterious effects of cis-urocanic acid and UVB radiation on Langerhans cells and on induction of contact hypersensitivity are mediated by tumor necrosis factor-alpha. J Invest Dermatol. 1992; 99:69S–70S. [PubMed: 1431236]
26. Guo A, Song B, Reid B, et al. Effects of physiological electric fields on migration of human dermal fibroblasts. J Invest Dermatol. 2010; 130:2320–7. [PubMed: 20410911]
27. Huang C, Jacobson K, Schaller MD. MAP kinases and cell migration. J Cell Sci. 2004; 117:4619–28. [PubMed: 15371522]

28. Mamalis A, Koo E, Isseroff RR, et al. Resveratrol Prevents High Fluence Red Light-Emitting Diode Reactive Oxygen Species-Mediated Photoinhibition of Human Skin Fibroblast Migration. PLoS One. 2015; 10:e0140628. [PubMed: 26488596]
29. Cho S, Lee MJ, Kim MS, et al. Infrared plus visible light and heat from natural sunlight participate in the expression of MMPs and type I procollagen as well as infiltration of inflammatory cell in human skin in vivo. J Dermatol Sci. 2008; 50:123–33. [PubMed: 18194849]
30. Kanazawa S, Fujiwara T, Matsuzaki S, et al. bFGF regulates PI3-kinase-Rac1-JNK pathway and promotes fibroblast migration in wound healing. PLoS One. 2010; 5:e12228. [PubMed: 20808927]
31. Li W, Fan J, Chen M, et al. Mechanism of human dermal fibroblast migration driven by type I collagen and platelet-derived growth factor-BB. Mol Biol Cell. 2004; 15:294–309. [PubMed: 14595114]
32. Sepe L, Ferrari MC, Cantarella C, et al. Ras activated ERK and PI3K pathways differentially affect directional movement of cultured fibroblasts. Cell Physiol Biochem. 2013; 31:123–42. [PubMed: 23363700]
33. Choi H, Lim W, Kim I, et al. Inflammatory cytokines are suppressed by light-emitting diode irradiation of P. gingivalis LPS-treated human gingival fibroblasts: inflammatory cytokine changes by LED irradiation. Lasers Med Sci. 2012; 27:459–67. [PubMed: 21814735]
34. Ong WK, Chen HF, Tsai CT, et al. The activation of directional stem cell motility by green light-emitting diode irradiation. Biomaterials. 2013; 34:1911–20. [PubMed: 23261211]
35. Stambolic V, Woodgett JR. Functional distinctions of protein kinase B/Akt isoforms defined by their influence on cell migration. Trends Cell Biol. 2006; 16:461–6. [PubMed: 16870447]
36. Vaidya RJ, Ray RM, Johnson LR. Akt-mediated GSK-3beta inhibition prevents migration of polyamine-depleted intestinal epithelial cells via Rac1. Cell Mol Life Sci. 2006; 63:2871–9. [PubMed: 17109063]
37. Yoeli-Lerner M, Yiu GK, Rabinovitz I, et al. Akt blocks breast cancer cell motility and invasion through the transcription factor NFAT. Mol Cell. 2005; 20:539–50. [PubMed: 16307918]
38. Gharbi SI, Zvelebil MJ, Shuttleworth SJ, et al. Exploring the specificity of the PI3K family inhibitor LY294002. Biochem J. 2007; 404:15–21. [PubMed: 17302559]
39. Sadick NS. Handheld LED array device in the treatment of acne vulgaris. J Drugs Dermatol. 2008; 7:347–50. [PubMed: 18459515]
40. Sadick NS. A study to determine the efficacy of a novel handheld light-emitting diode device in the treatment of photoaged skin. J Cosmet Dermatol. 2008; 7:263–7. [PubMed: 19146602]

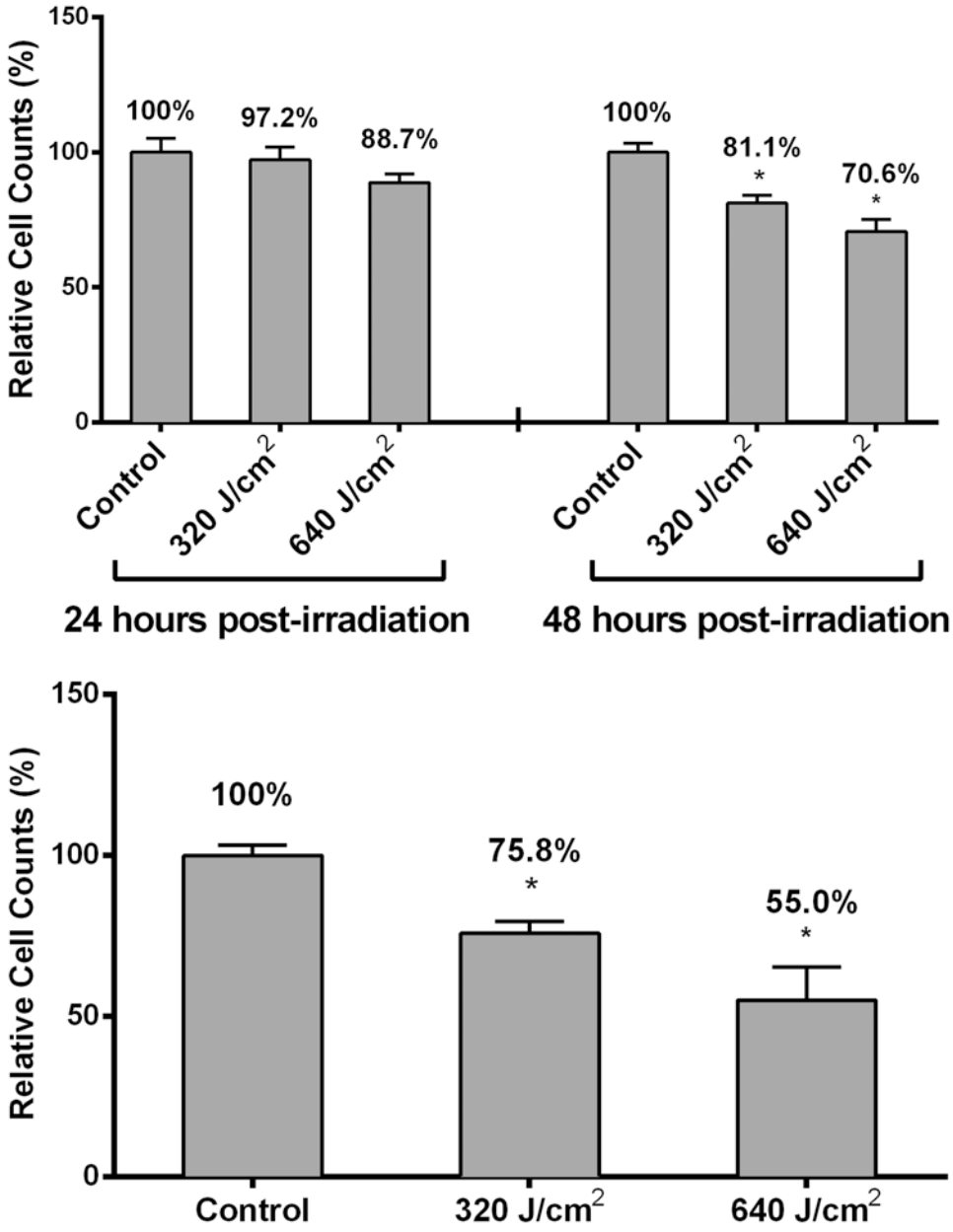

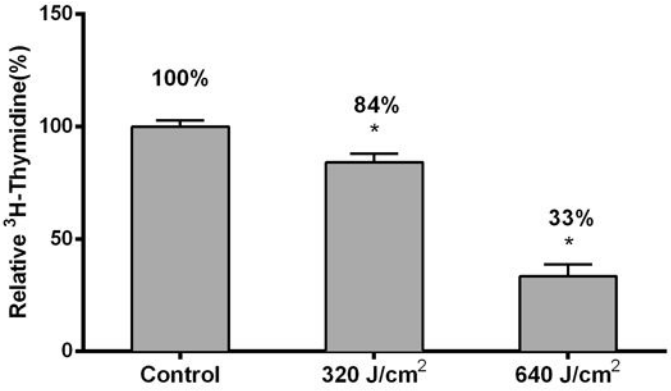

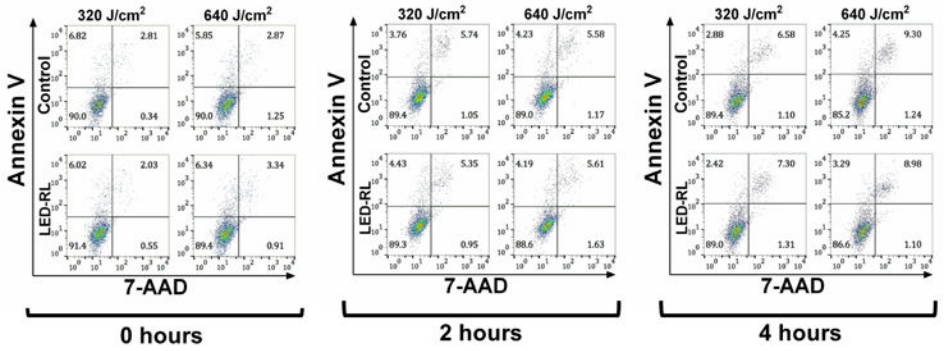

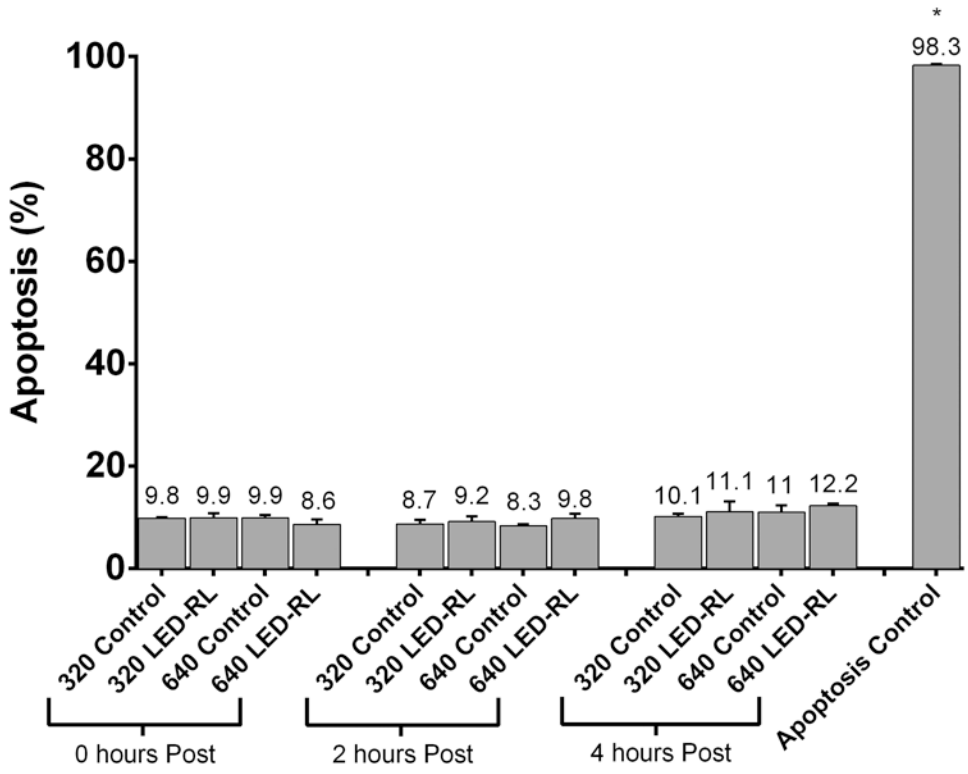

Figure 1.

High Fluence LED-RL (633 nm) decreases human dermal fibroblast cell count and proliferation in a dose-dependent manner without increasing apoptosis. (a) DHFs irradiated with 320 and 640 J/cm2 LED-RL were incubated for 24 or 48 hours and then counted using the trypan blue exclusion assay. Cells counts of groups treated with HF-LED-RL were compared to matched control dishes to calculate relative cell count, a surrogate of cell proliferation. 320 and 640 J/cm2 LED-RL decreased relative cell count to 97.2 ± 4.7% ($p=0.616$) and 88.7 ± 3.3% ($p = 0.043$) compared to matched controls, respectively. DHFs irradiated with 320 and 640 J/cm2 LED-RL and then incubated for 48 hours demonstrated decreased relative cell count to 81.0 ± 2.9% ($p < 0.001$) and 70.6 ± 4.5% ($p < 0.001$) compared to matched controls, respectively.

(b) DHFs irradiated with 320 and 640 J/cm2 LED-RL every 12 hours for a total of 4 total doses were collected 48 hours following the first LED-RL dose and counted using the trypan blue exclusion assay. Cells counts of groups treated with HF-LED-RL were compared to matched control dishes to calculate relative cell count, a surrogate of cell proliferation. Multiple doses of 320 and 640 J/cm2 LED-RL significantly decreased relative cell count to 75.8 ± 3.6% ($p = 0.006$) and 55.0 ± 10.3% ($p < 0.001$) compared to matched controls, respectively.

(c) DHFs irradiated with 320 and 640 J/cm2 LED-RL and then incubated for 18 hours with 4 μCi of tritiated thymidine (3H-Thy). The relative 3H-Thy incorporation of treated dishes was compared to matched control dishes as a surrogate of proliferation rate. 320 and 640 J/cm2 LED-RL decreased relative 3H-Thy incorporation to 84.2 ± 3.8% ($p=0.003$) and 33.4 ± 5.3% ($p < 0.001$) compared to matched controls, respectively.

(d) Representative Annexin V vs. 7-AAD flow cytometry plots 0 hours, 2 hours, and 4 hours post-irradiation.

(e) HF-LED-RL (633 nm) does not induce significant increases in total apoptosis levels at 0, 2, or 4 hours post-irradiation in HDFs. Bars represent average percent AV positive cells in each treatment group. For purposes of comparison to a positive control, we used temperature (50°C) to induce apoptosis levels of 98.3%. Error bars represent standard error of the mean. Data are representative of three repeat experiments in two different HDF strains. Similar temporal results were obtained in the two strains examined. Error bars represent mean ± SEM; *P<0.05

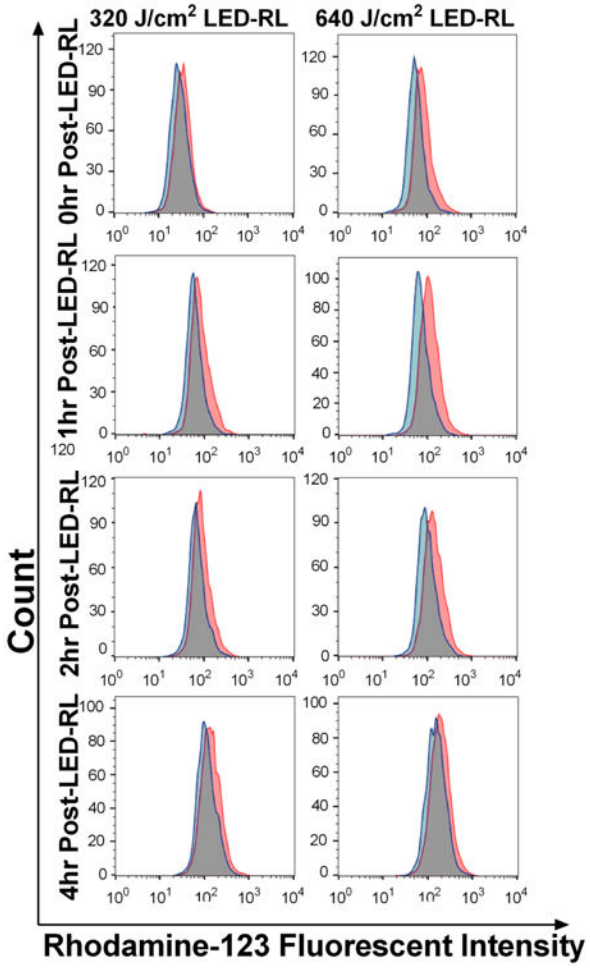

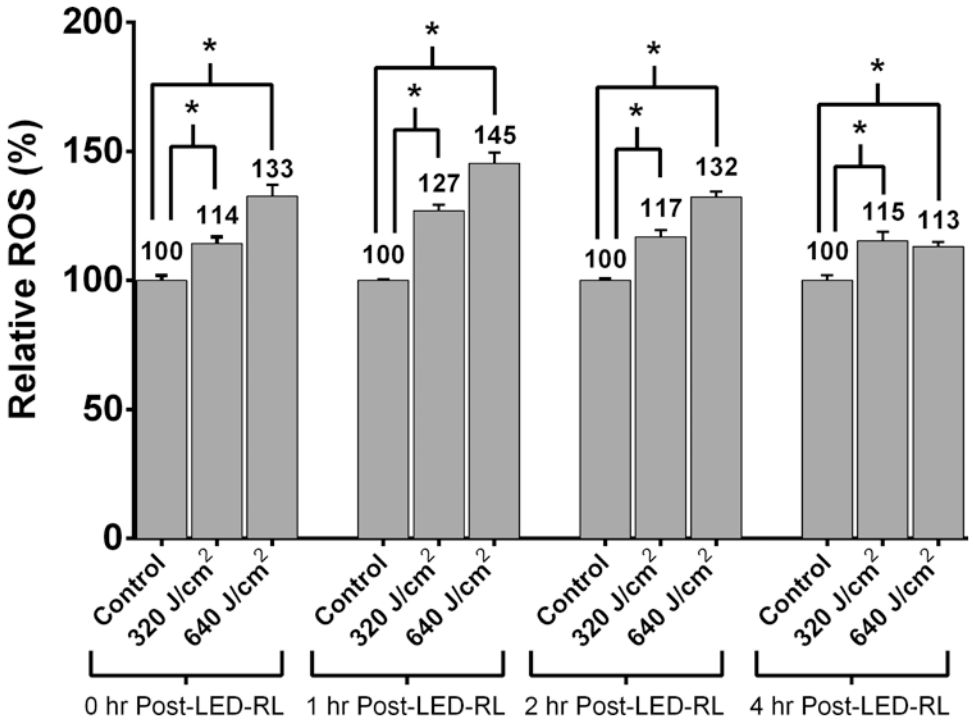

Figure 2.

HDFs treated with 320 and 640 J/cm2 LED-RL demonstrate significantly increased ROS levels compared to matched controls for up to 4 hours post-irradiation. (a) Representative flow cytometry curves. Red curves represent mean fluorescent intensity of HDFs treated with HF-LED-RL, blue curves represent matched controls.

(b) At 0, 1, 2, and 4 hours following irradiation, ROS levels were significantly elevated compared to matched controls. Peak ROS levels were observed 1 hour following 320 and 640 J/cm2 LED-RL and found to be 127% (p=0.0026) and 145% (p=0.0018) relative to matched controls, respectively. Data are representative of three repeat experiments in two different HDF strains. Similar temporal results were obtained in the two strains examined. Error bars represent mean ± SEM; *P<0.05

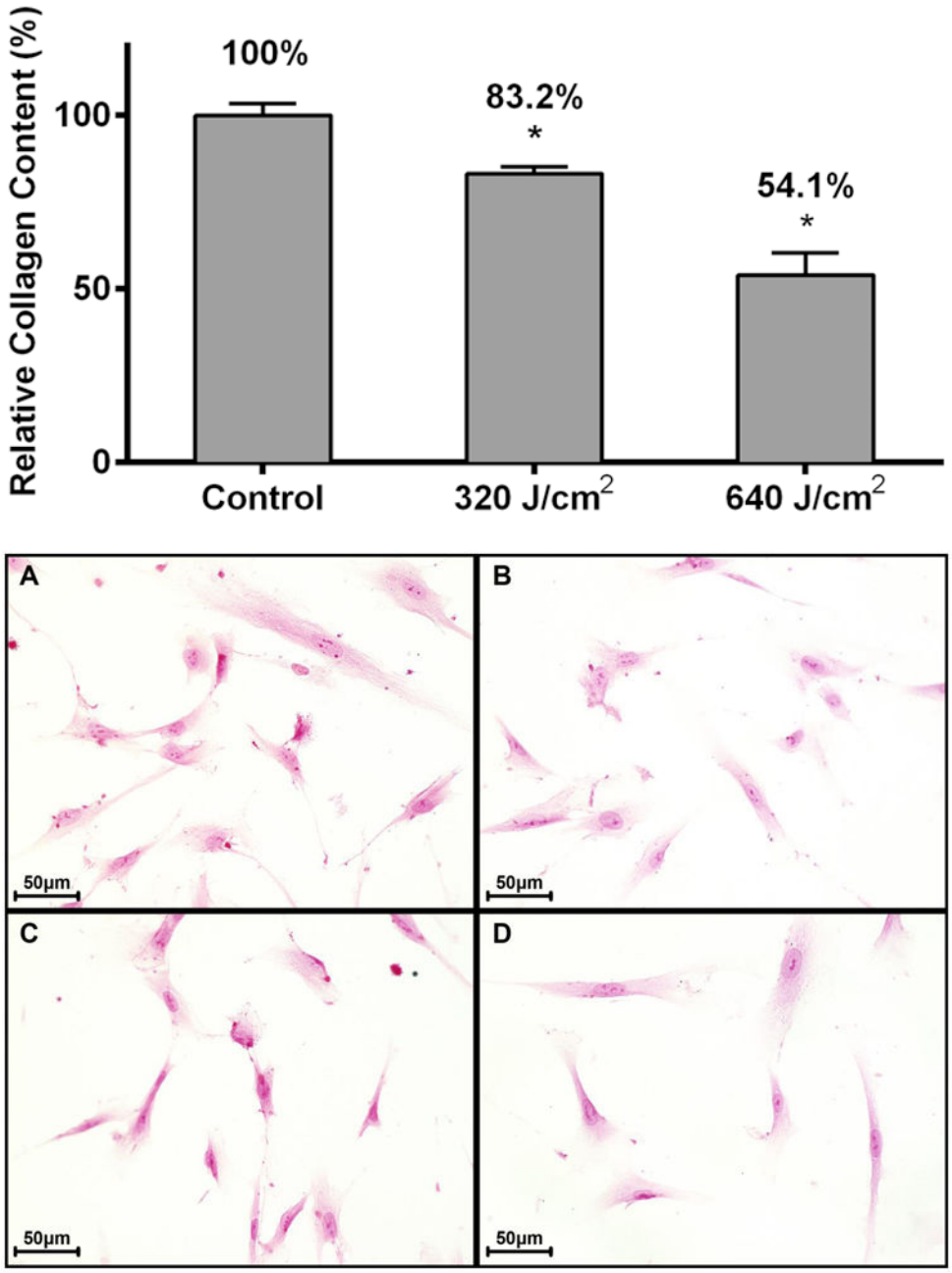

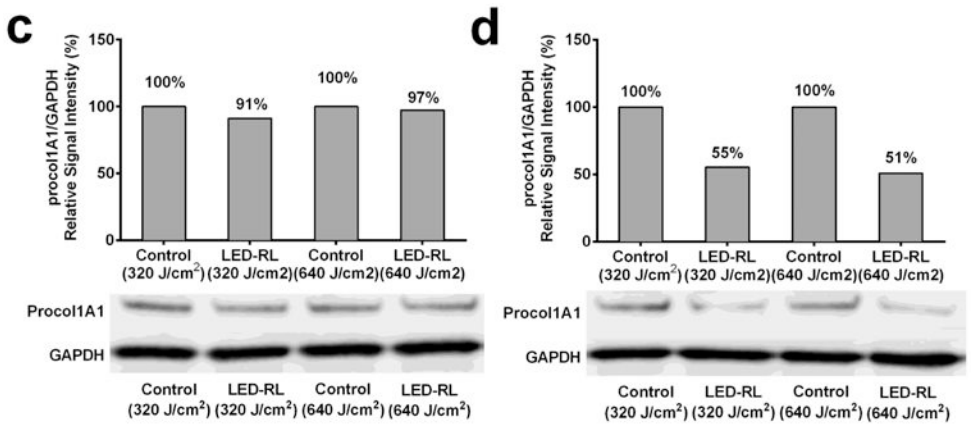

Figure 3.

High Fluence LED-RL inhibits human dermal fibroblast collagen production.HDFs were irradiated, fixed, and stained with picrosirius red (a collagen-specific dye). Picrosirius red was then eluted and measured using spectrophotometry. HF-LED-RL irradiated groups demonstrated a dose-dependent decrease in collagen levels with 320 J/cm2 = 83.2 ± 2.0% of matched control (p=0.002), 640 J/cm2 = 54.1 ± 6.3% of matched control ($p < 0.001$).

(b) HDFs treated with HF-LED-RL and stained with picrosirius red demonstrated a decrease in staining intensity compared with matched controls when viewed with light microscopy at 40x magnification. (A, top left panel) Control for 320 J/cm2 LED-RL. (B, top right panel) Treatment group irradiated with 320 J/cm2 LED-RL. (C, bottom left panel) Control for 640 J/cm2 LED-RL. (D, bottom right panel) Treatment group irradiated with 640 J/cm2 LED-RL.

(c) Western blot staining of HDFs treated with HF-LED-RL demonstrated no significant decrease in procol1A1 levels immediately following irradiation. A representative western blot is shown. After normalizing to GAPDH, we found 320 J/cm2 LED-RL resulted in 91% procol1A1 and 640 J/cm2 LED-RL resulted in 97% procol1A1, relative to matched controls, respectively. (d) Western blot staining of HDFs treated with HF-LED-RL demonstrated a decrease in procol1A1 levels at 2 hours following irradiation. A representative western blot is shown. After normalizing to GAPDH, we found 320 J/cm2 LED-RL resulted in 55% procol1A1 and 640 J/cm2 LED-RL resulted in 51% procol1A1, relative to matched controls, respectively. Data are representative of three repeat experiments in two different HDF strains. Similar temporal results were obtained in the two strains examined. Error bars represent mean ± SEM; *P<0.05

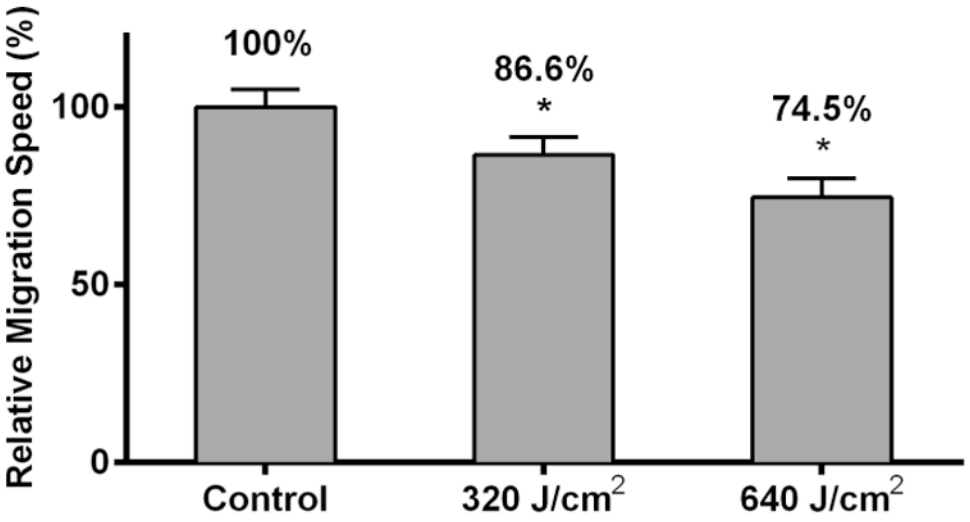

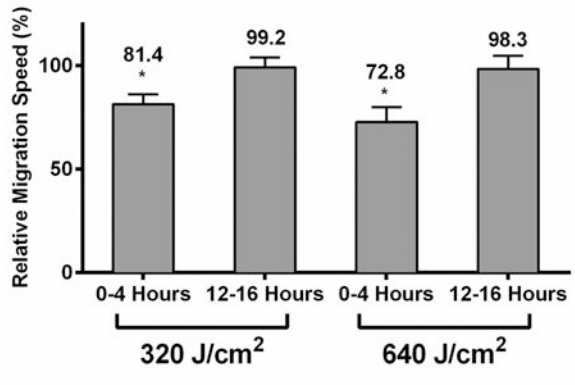

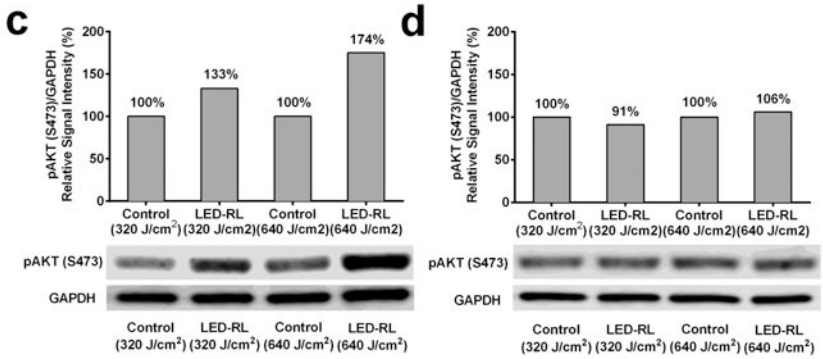

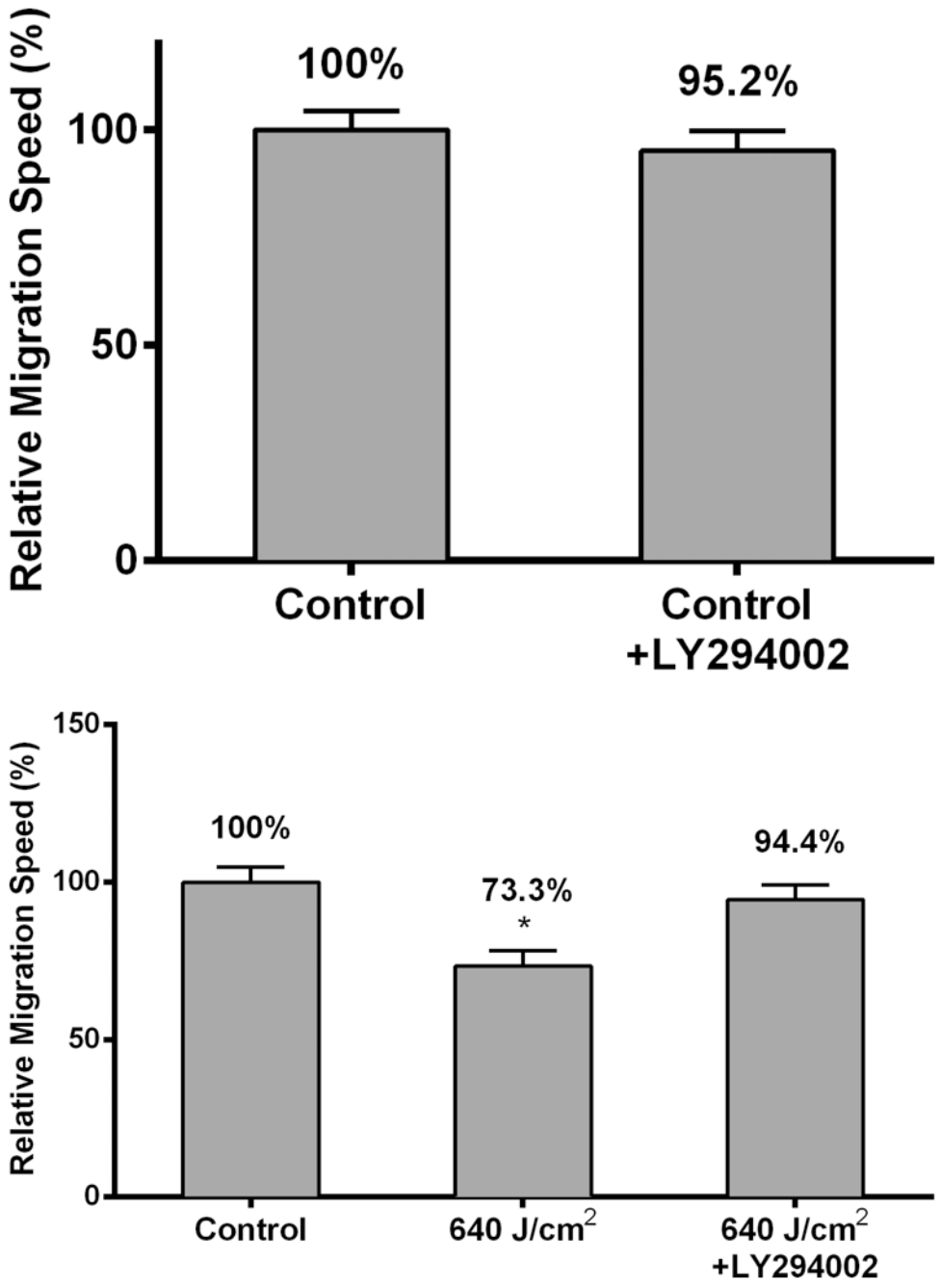

Figure 4.

HF-LED-RL inhibits human dermal fibroblast migration speed through modulation of the PI3K/AKT pathway. (a) HDF migration speed following HF-LED-RL irradiation was assessed used time-lapse video microscopy. HF-LED-RL fluences of 320 and 640 J/cm2 decreased HDF migration speed to 86.6% ($p < 0.001$) and 74.5% ($p<0.001$) relative to matched controls, respectively.

(b) High Fluence LED-RL significantly decreases the migrations speed of HDFs for up to 12 hours. 320 and 640 J/cm2 of LED-RL resulted in significantly decreased migration speed relative to matched control for 12-hours after irradiation when measured at 4 hour intervals.

Pictured above, relative cellular migration speed for HDFs treated with 320 J/cm2 at 0-4 hours was 81.4 ± 4.8% ($p<0.05$) and at 12-16 hours was 99.2 ± 4.8%. HDFs treated with 640 J/cm2 at 0-4 hours was 72.8 ± 7.1% ($p<0.05$) and at 12-16 hours was 98.3 ± 6.5%.
(c) HDFs treated with 320 and 640 J/cm2 LED-RL demonstrated increased AKT phosphorylation (S473) compared to matched controls at 4 hours post-irradiation. A representative western blot is shown. (d) AKT phosphorylation was no longer increased at 12 hours post-irradiation. A representative western blot is shown.
(e) Pretreatment with 30 μM LY294002 (antagonist of AKT phosphorylation) did not significantly alter HDF migration speed when compared with control. Pretreating HDFs with 30 μM LY294002 for 30 minutes resulted in a relative speed of 95.2 ± 4.7% ($p = 0.48$) compared to untreated control.
(f) Pretreatment with 30 μM LY294002 (antagonist of AKT phosphorylation) prevented the inhibitory effects of 640 J/cm2 LED-RL on HDF migration speed. Primary HDFs with or without Ly294002 were treated with HF-LED-RL and their migration speed was assessed used time-lapse video microscopy. 640 J/cm2 LED-RL significantly decreased migration speed (73.3 ± 4.9%, $p < 0.0001$) versus matched control. Pretreating HDFs with 30 μM LY294002 for 30 minutes blocked the inhibitory effects of 640 J/cm2 LED-RL on migration resulting in a relative speed of 94.4 ± 4.8% ($p = 0.62$) relative to matched control pretreated with 30 μM LY294002.Data are representative of three repeat experiments in two different HDF strains. Similar temporal results were obtained in the two strains examined. Error bars represent mean ± SEM; *$P<0.05$.